

N92-27816

THE LARGE-ANGLE MAGNETIC SUSPENSION TEST FIXTURE

Colin P. Britcher, Mehran Ghofrani

Department of Mechanical Engineering and Mechanics, Old Dominion University

Thomas C. Britton

Lockheed Engineering and Sciences Company

Nelson J. Groom

Spacecraft Controls Branch, NASA Langley Research Center

INTRODUCTION

As part of a NASA effort to develop the technology and techniques required to demonstrate the magnetic suspension of objects over wide ranges of attitudes, a small-scale demonstration project has been undertaken. The objectives here are to suspend a cylindrical element containing a permanent magnet core, to demonstrate stability and control in five degrees-of-freedom, and to permit controlled rotation of the model in one degree-of-freedom over the full range of 360 degrees. Further constraints are that all suspension and control electromagnets are to be behind a flat plane, located some distance from the model. Since this is a ground-based experiment and in order to maintain generality, the plane is chosen to be horizontal with the model levitated above the plane by repulsive forces.

Potential applications for large-gap magnetic suspension systems capable of controlled excursions through large angular ranges include the manipulation and pointing of space payloads, microgravity vibration isolation and the suspension of models in wind tunnels. Indeed, controlled suspension of a model through an angular (angle-of-attack) range of around 100° has already been demonstrated in a wind tunnel system [1].

Design studies for a hypothetical large-scale system were undertaken in 1987-88 [2,3,4]. The specifications for this system required that a model be "levitated" above a clear floor surface and be capable of being oriented arbitrarily in azimuth. The air-gap (between model and electromagnets) was very large, around 1 meter. Several approaches were examined, with all studies concluding that such a device was feasible, at least insofar as electromagnets of appropriate size were within current technological limits. The most promising of these early concepts appeared to be the arrangement of several electromagnets in a flat or "planar" array, a configuration studied by several groups. Madison Magnetics Incorporated (MMI) [4] suggested a geometry refined to a circular quasi-axisymmetric arrangement of five electromagnets, since the principal model rotation

required was about the vertical axis (the axis of the circular array) and it is clear that a minimum of five electromagnets are required for control in five degrees-of-freedom.

The principal uncertainty in this design was the control of the model, particularly over the wide range of orientation. A suspension system of this particular type had not been attempted before, since various design features were quite unusual :

i) "Levitation" entirely by repulsive forces (attractive forces usually employed).

ii) No attempt to "decouple" electromagnets (normally the electromagnet configuration is developed so as to provide at least some natural decoupling between degrees-of-freedom).

It was therefore decided to proceed with design and construction of a small-scale proof-of-concept demonstration system, in order to verify the feasibility of this design approach and to permit control system development. It was decided to follow the MMI design in general layout, but with a levitation height (air gap between electromagnets and model) reduced to 0.1 meters. This configuration is illustrated in Figure 1.

HARDWARE DESCRIPTION

An array of five, room temperature, copper electromagnets are distributed evenly on a 13.77 cm radius. The coils are wound with 509 turns of AWG 10 enamelled copper wire on bakelite forms, with iron cores. There is no provision for active cooling, it being felt that operation of the LAMSTF would be rather intermittent in nature. The design maximum steady-state current is around 15 Amperes (Coil 1), limited by the coil temperature rise. At 15 Amps, the temperature rise is around 1.5°C/minute, giving perhaps 30 minutes useful run-time. Temperature sensors with over-temperature alarms and power cut-outs are also fitted. The electromagnets are mounted on a heavy aluminum plate 1.27 cm (0.5 inches) thick. The electromagnet assembly is illustrated in Figure 2.

The suspended element consists of 16 wafers, 0.3135 cm long (0.1235 inches) and 0.7963 cm diameter (0.3135 inches) of Neodymium-Iron-Boron (Nd-Fe-B) permanent magnet material epoxied into an aluminum tube, 5.32 cm long (2.095 inches) and 0.9525 cm (0.375 inches) outside diameter. The estimated magnet mass is 20.03 grams (by subtracting the alloy tube weight from the total). The total model mass is 22.5 grams. The moment of inertia about the transverse axis was measured with a bifilar pendulum technique and found to be 5.508×10^{-6} kg.m².

The position sensing system follows traditional wind tunnel MSBS practice of multiple light beams partially interrupted by the model. The beams are arranged in two orthogonal planes (vertical and horizontal) in this case. The light sources are miniature infra-red light-emitting

diodes, intended for use with fiber-optics. The light receivers are matching infra-red phototransistors. Due to the beam dispersion of around 20 degrees (included cone angle) from the transmitter, miniature plano-convex collimating lenses (6 mm diameter and 12 mm focal length) were added to both transmitter and receiver, primarily in order to increase the signal level at the receiver. Also, some care was taken to shield and screen the light path. The complete sensor system is mounted on a framework which is initially fixed in one orientation relative to the suspension electromagnets. However, the design permits rotation of the framework about a vertical axis, either manually, or by some form of motor drive to be added later. A schematic diagram of the assembly is shown in Figure 3, and the installation of the sensors on the electromagnet array is shown in Figure 4.

To facilitate early commissioning of the LAMSTF system, an analog controller was constructed, again following traditional wind tunnel MSBS practice. Position sensor signals are summed-and-differenced, where appropriate, to derive motion signals in the five model degrees of freedom required, that is: axial, lateral, and vertical translation and pitch and yaw rotations. Each signal passes through conventional, dual, series phase-advance compensators. A marked departure from previous controllers is the incorporation of extensive decoupling at the output of the controller, discussed more fully later. A block diagram of the controller and outlines of the circuitry employed is shown in Figure 5. An important difficulty to be overcome by the controller is stabilization of the three unstable modes of motion, found in this type of suspension system [5], illustrated in Figure 6. The most important modes are the so-called "compass needle" modes, where the model is attempting to reverse its direction in the axial component of applied field. The natural frequency is quite high in this application, around 10 Hz. The controller must overcome this instability and provide the appropriate stiffness and damping.

Each electromagnet is driven by a transistor switching power amplifier, rated at $\pm 150V$ and $\pm 30A$ continuous, up to 60A peak with full four-quadrant operation. The switching frequency is 22kHz. Six amplifiers, with associated D.C. power supplies and control electronics are installed as shown in Figure 7.

HARDWARE PERFORMANCE

Each electromagnet has a resistance of around 0.74Ω , not including connecting leads, and an inductance of around 27.5 mH, with iron cores present. Mutual inductances are estimated at 1.6 mH and 0.37 mH, adjacent and non-adjacent electromagnets respectively. There is some uncertainty and ambiguity in the inductance values, due to eddy current effects discussed below.

If flux from an electromagnet penetrates a conducting medium, eddy currents will be

generated in that medium when the current in the electromagnet is varied. This is of some concern in magnetic suspension applications since control of the suspended or levitated object is generally maintained by constant adjustment of the electromagnet currents. If eddy currents are generated during these adjustments, then the rate of change of field at the model (corresponding to the rate of application of forces and moments) might be reduced, or subject to a phase lag. The mounting of the five LAMSTF electromagnets on a heavy aluminum plate was intended to permit a full assessment of the effects of eddy currents on suspension stability.

Following a simplified approach, wherein the eddy current circuit is supposed to be invariant with excitation frequency, it can be shown that the terminal characteristics of the electromagnet will be as follows :

$$V = I \left(\frac{R + (L + \frac{R}{R_e} L_e) s + (\frac{L L_e - L_m^2}{R_e}) s^2}{1 + \frac{L_e}{R_e} s} \right) \quad - (1)$$

where R_e , L_e are the resistance and inductance of the eddy current circuit and L_m is the mutual inductance between primary (electromagnet coil) and secondary. Continuing, the field components generated (at the suspended object) can be expressed as

$$B = I \left(k + \frac{k_e L_m s}{R_e + L_e s} \right) \quad - (2)$$

where k , k_e are constants representing the field generated at the suspension location by the electromagnet and the eddy current respectively. The break frequency is clearly the inverse of the time constant of the eddy current circuit. It is argued in this application that the factors k_e , L_e/R_e and L_m can be estimated by geometrical analysis and by careful measurements of electromagnet terminal characteristics. An obvious objection to this representation is the fact that the penetration depth (skin depth) of eddy currents will decrease with increasing frequency, leading to changes in eddy current circuit resistance and so forth. However, the frequencies of interest in this application are quite low, so that this effect will be small.

Measurements of the terminal characteristics of a LAMSTF coil are summarized in Figure 8, with typical results of calculations based on Equation (1). Careful comparison reveals a significant phase defect from ideal, centered around the natural frequency of the eddy current circuit. The actual electromagnets show two separate defects, one at a relatively low frequency, related to currents in the alloy plate, and another at a much higher frequency, due to the (unlaminated) iron core.

The magnetic field generated by each electromagnet has been calculated using the computer program VF/GFUN. This uses an integral equation formulation, only requiring discretization of the iron regions in a problem. Some field measurements have been made to validate the computations, with acceptable overall agreement. The set of field and field gradient components generated at the model centroid have been calculated and are presented in Table A below. It should be noted that these values are for a single isolated coil and core. There is some evidence of magnetization of adjacent cores, resulting in small distortions of these fields.

TABLE A - Computed field and field gradients from a single coil
(1 Amp, Tesla and Tesla/meter $\times 10^{-6}$)

Coil#	B _x	B _y	B _z	B _{xx}	B _{xy}	B _{xz}
1	240.9	0	-106.3	2118.2	0	-2852.7
2	74.4	229.1	-106.3	-1289.4	1107.2	-881.5
3	-194.9	141.6	-106.3	816.6	-1791.5	2307.9
4	-194.9	-141.6	-106.3	816.6	1791.5	2307.9
5	74.4	-229.1	-106.3	-1289.4	-1107.2	-881.5

Following Reference 6, and restricting the model orientation to the datum, torques and forces are related to applied fields and gradients in the following way :

$$\begin{bmatrix} T_y \\ T_z \\ F_x \\ F_y \\ F_z \end{bmatrix} = \text{Vol } M_{\bar{x}} \begin{bmatrix} -B_{z_1} & -B_{z_2} & -B_{z_3} & -B_{z_4} & -B_{z_5} \\ B_{y_1} & \ddots & & & \\ B_{xx_1} & & \ddots & & \\ B_{xy_1} & & & \ddots & \\ B_{xz_1} & & & & \ddots \end{bmatrix} \begin{bmatrix} I_1 \\ \vdots \\ I_5 \end{bmatrix} \quad - (3)$$

The coefficients B_{z_1} etc., are as given in Table A. By setting each element of the left-hand side vector to a non-zero value in turn, with all other values zero, the required current distributions to generate each force or moment component independently can be deduced from the normalized current vectors resulting.

$$\begin{bmatrix} I_1 \\ I_2 \\ I_3 \\ I_4 \\ I_5 \end{bmatrix} = \begin{bmatrix} 0.625 & 0 & 1 & 0 & 1 \\ 1 & 1 & -0.809 & 0.618 & 0.309 \\ 0.768 & 0.618 & 0.309 & 1 & -0.809 \\ 0.768 & -0.618 & 0.309 & 1 & -0.809 \\ 1 & -1 & -0.809 & -0.618 & 0.309 \end{bmatrix} \begin{bmatrix} T_{y \text{ demand}} \\ T_{z \text{ demand}} \\ F_{x \text{ demand}} \\ F_{y \text{ demand}} \\ F_{z \text{ demand}} \end{bmatrix} \quad - (4)$$

By use of this demand allocation matrix, the control system is statically decoupled into model degrees of freedom. There are still dynamic couplings, due to the natural modes of motion, as discussed in [5], chiefly a coupling from axial motion into pitch. The supposition is, of course, that if these couplings are weak enough they simply appear as disturbances to the relevant degrees-of-freedom of the controller. The demand allocation matrix is implemented by the the circuitry illustrated in Figure 5, by appropriate selection or setting of input resistors to the summers.

Using best estimates of model mass, core volume and magnetization, the equilibrium levitation currents can also be found :

$$\text{Vol} = 2.498 \times 10^{-6} \text{ m}^3; \quad M_{\bar{x}} = 955,000 \text{ A/m (1.2 Tesla);} \quad F_z = 0.221 \text{ N}$$

The required B_{xz} is found to be 0.0926 T/m. Directly from Equation 4, the equilibrium suspension currents should therefore be

$$(I_1, I_2, I_3, I_4, I_5) = (-12.984, -4.012, 10.504, 10.504, -4.012)$$

Preliminary suspension tests, such as shown in Figure 9, have shown currents of

$$(I_1, I_2, I_3, I_4, I_5) = (-15.5, -5.9, 12.4, 12.1, -5.9)$$

- which is reasonable agreement, considering the large number of estimated or computed values involved.

DIGITAL CONTROLLER

The analog controller was only intended to permit demonstration of suspension, preliminary operation, and hardware checkout and characterization. Due to the variation of coupling coefficients (equations 3,4) with yaw orientation, a digital controller with adaptive decoupling is essential for demonstration of 360° yaw rotation. The calculation and adaptation will follow the procedures outlined in References 5,7.

The control approach being followed is based on Linear Quadratic Gaussian (LQG) control theory. A Kalman filter is used to provide state estimates (position, orientation and corresponding rates) for input to an Integral Feedback Regulator. Feedback gain matrices have been obtained from a discrete-time simulation of the controller, which has been developed using MatrixX/SystemBuild. This control synthesis approach follows work contained in Reference 7. The hardware configuration, illustrated in Figure 10, consists of a data acquisition system, hosted by a PC-XT class controller, communicating with 68020/68881 computer through dual-port RAM. The A/D and D/A converters are all 12-bit types, communicating with the LAMSTF hardware through current-loop interfaces. Control hardware is presently complete and software is nearing completion. The digital controller will be installed immediately upon completion.

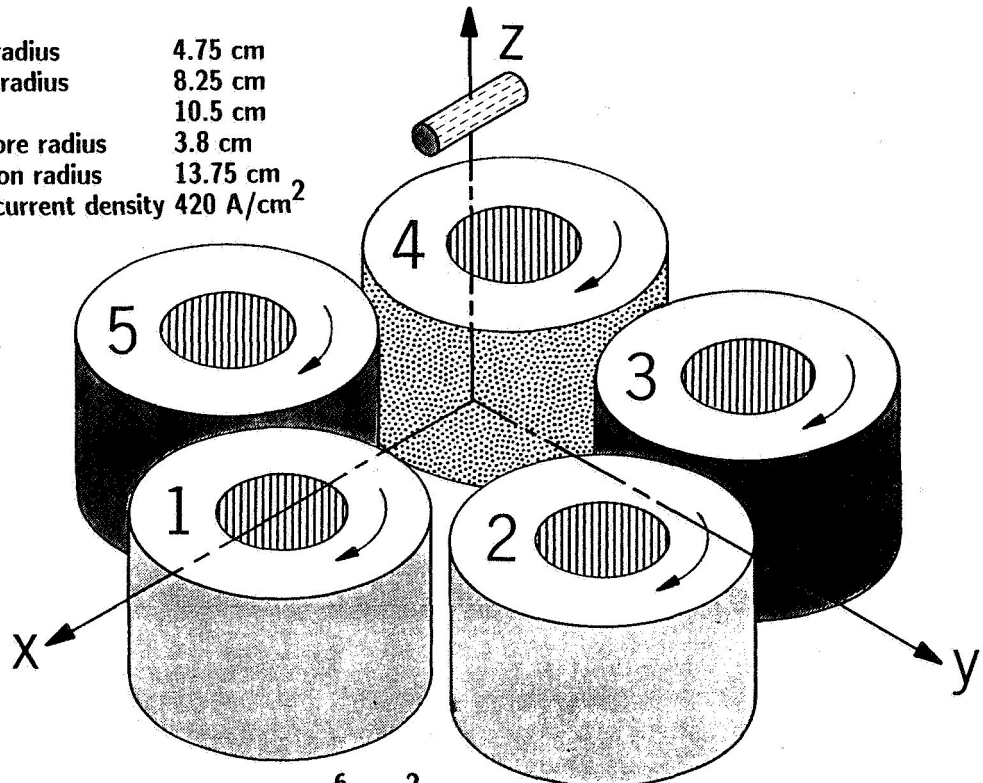
ACKNOWLEDGEMENTS

This work was partially supported by NASA Grant NAG-1-1056, Technical Monitor, Nelson J. Groom.

REFERENCES

1. Parker, D.H.: Techniques for Extreme Attitude Suspension of a Wind Tunnel Model in a Magnetic Suspension and Balance System. NASA CR-181895, October 1989.
2. Groom, N.J.: Description of the Large-Gap Magnetic Suspension System (LGMSS) Ground-Based Experiment. Technology 2000. NASA CP-3109, Vol.2, pp.365-377, March 1991.
3. Britcher, C.P.: Technical Background for a Magnetic Levitation System. NASA CR-178301, May 1987.
4. Boom, R.W.; Abdelsalam, M.K.; Eyssa, Y.M.; McIntosh, G.E.: Repulsive Force Support System Feasibility Study. NASA CR-178400, October 1987.
5. Groom, N.J.; Britcher, C.P.: Stability Considerations for Magnetic Suspension Systems using Electromagnets Mounted in a Planar Array. NASA CP-10066, Vol.1, pp.355-376, March 1991.
6. Groom, N.J.: Analytical Model of a Five Degree of Freedom Magnetic Suspension and Positioning System. NASA TM-100671, March 1989.
7. Groom, N.J.; Schaffner, P.R.: An LQR Controller Design Approach for Large-Gap Magnetic Suspension Systems (LGMSS). NASA TM-101606, July 1990.

Inner radius 4.75 cm
 Outer radius 8.25 cm
 Depth 10.5 cm
 Iron core radius 3.8 cm
 Location radius 13.75 cm
 Max. current density 420 A/cm²



Model 0.0225kg, $5.5 \times 10^{-6} \text{kg m}^2$
 Permanent magnet 0.008m diameter, 0.05m, 1.2 Tesla

Figure 1 - Large-Angle Magnetic Suspension Test Fixture (LAMSTF) Configuration

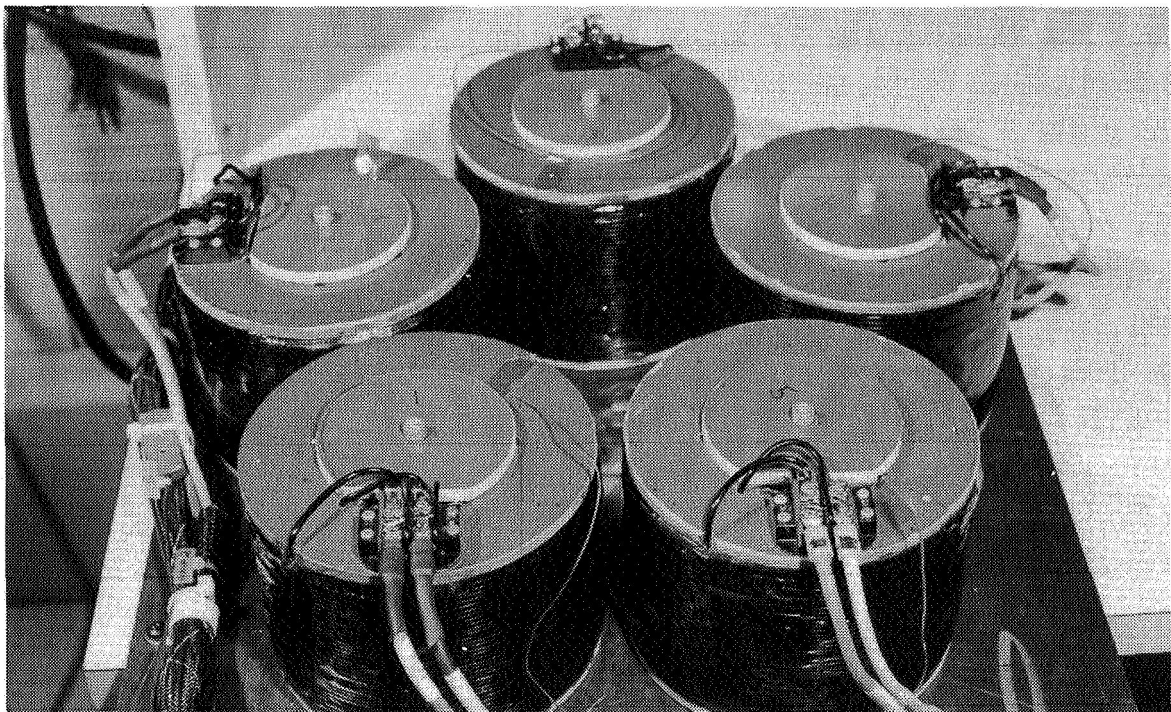


Figure 2 - LAMSTF Electromagnet Assembly

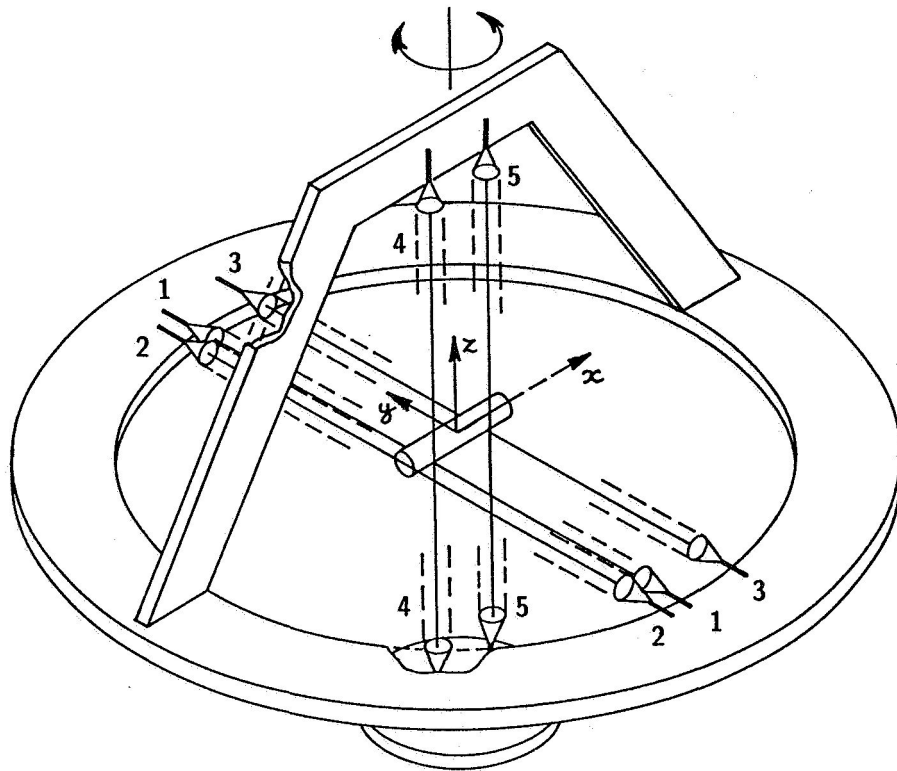


Figure 3 - Sensing System Schematic

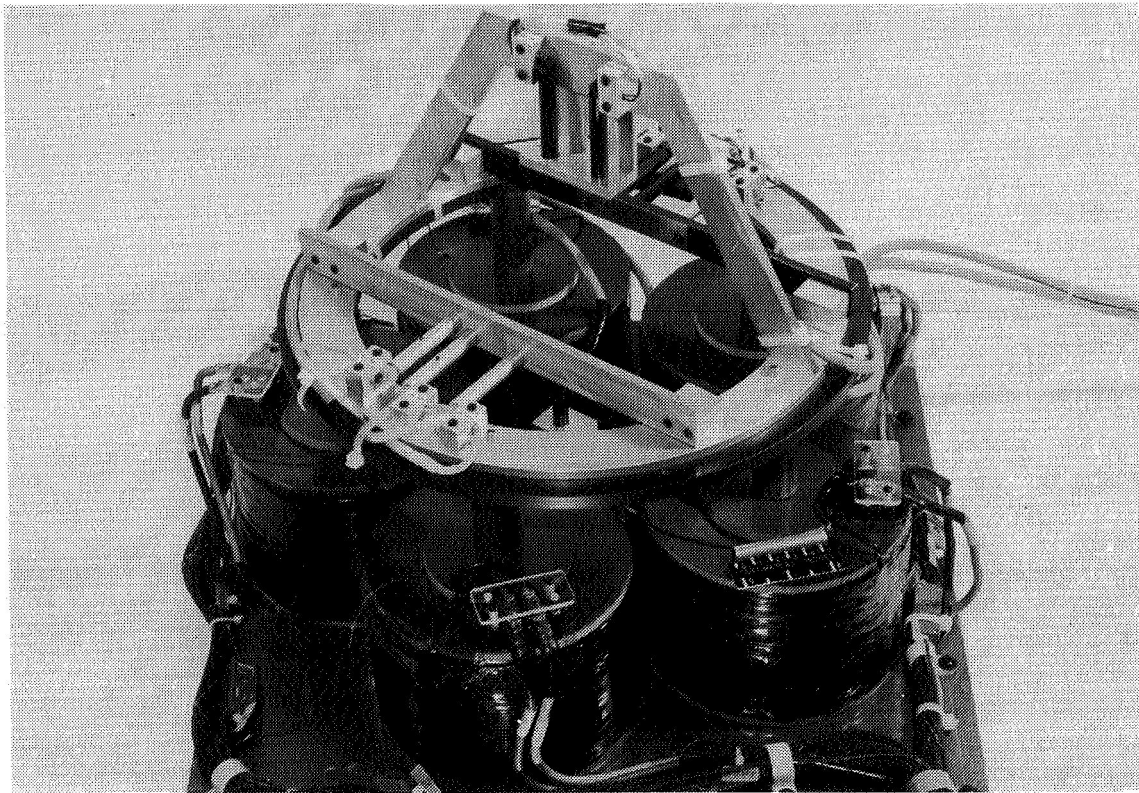


Figure 4 - Sensing System Installed on Electromagnet Assembly

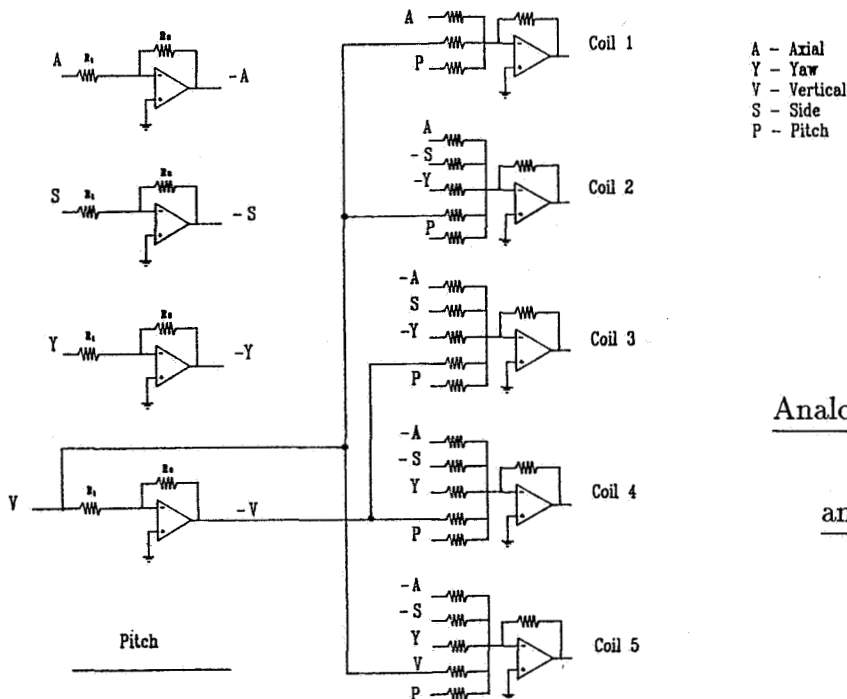
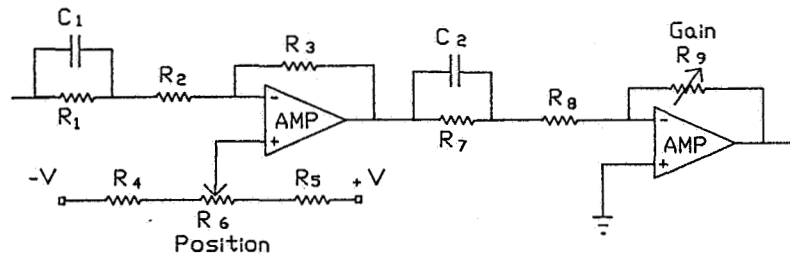
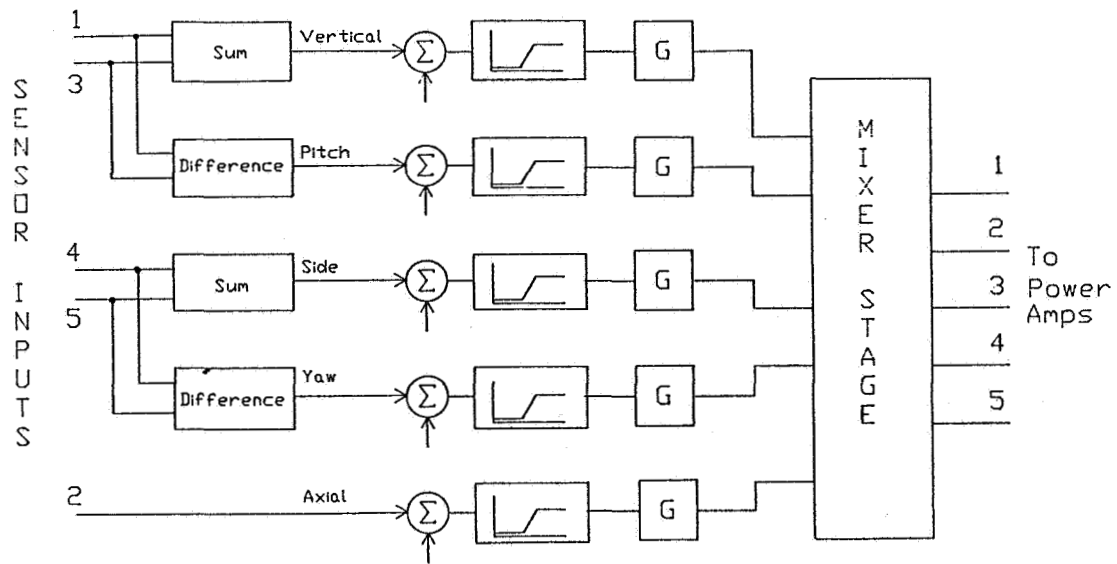


Figure 5

Analog Controller Block Diagram (top)

and Circuit Details (bottom)

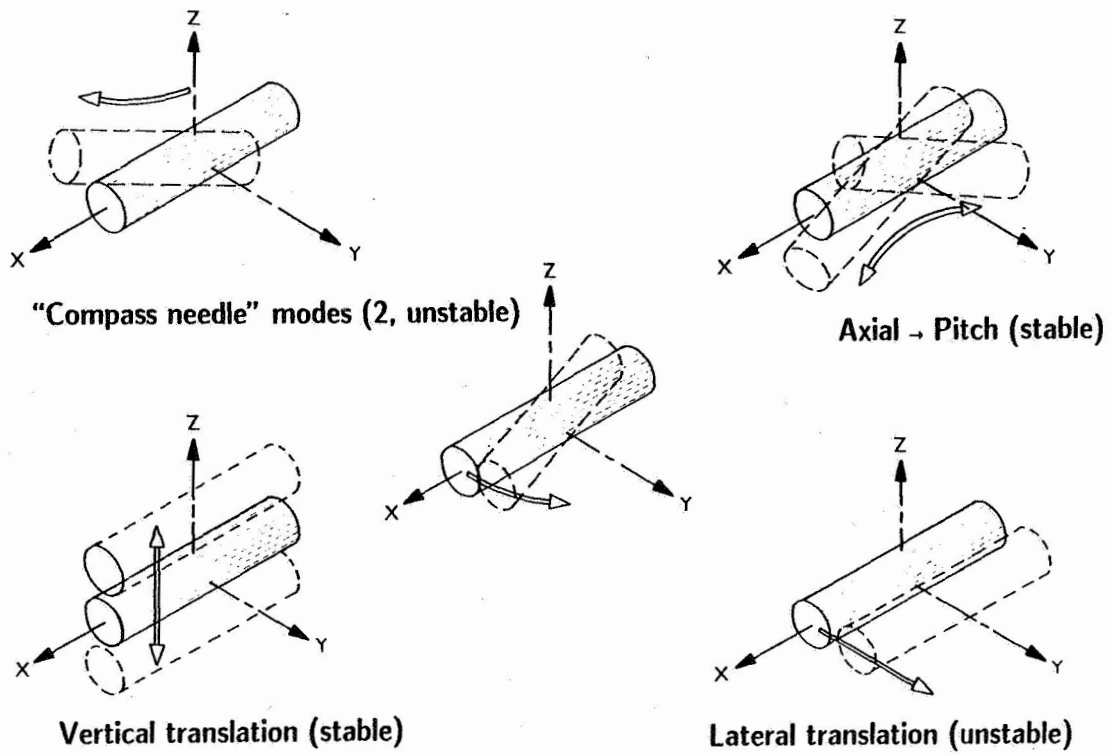


Figure 6 - Natural Modes of Suspended Element

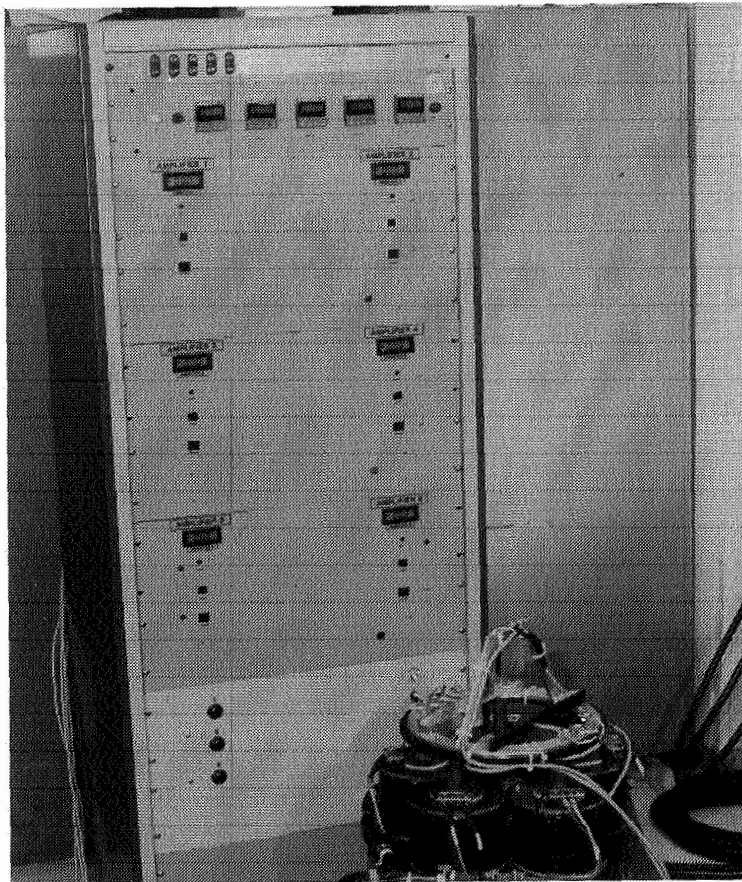


Figure 7 - LAMSTF Power

Supply Assembly

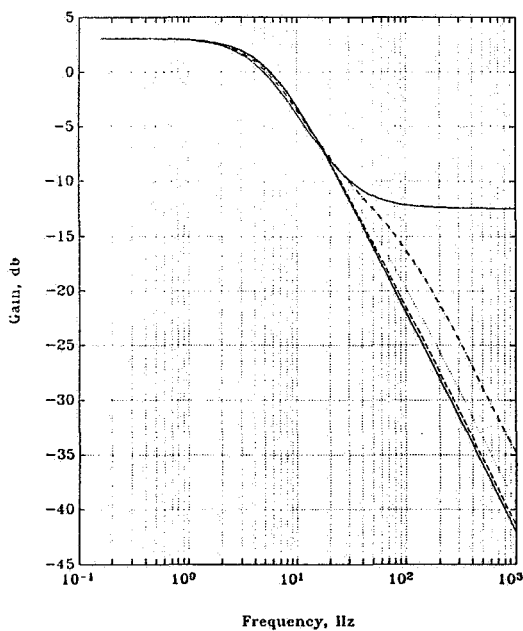
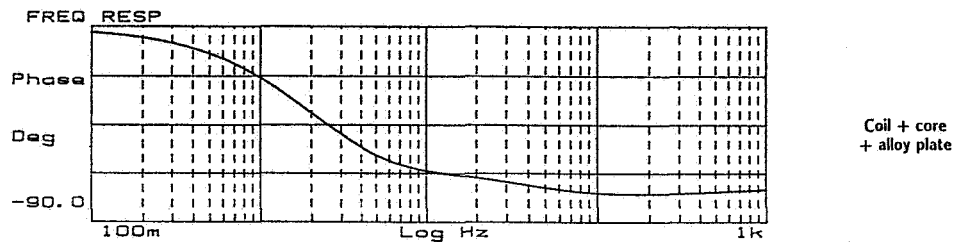
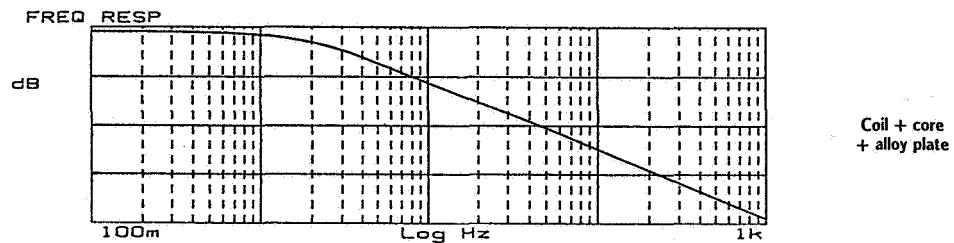


Figure 8 - Coil Terminal Characteristics

LAMSTF coil (top) and single time-constant model (bottom, using Equation 1)

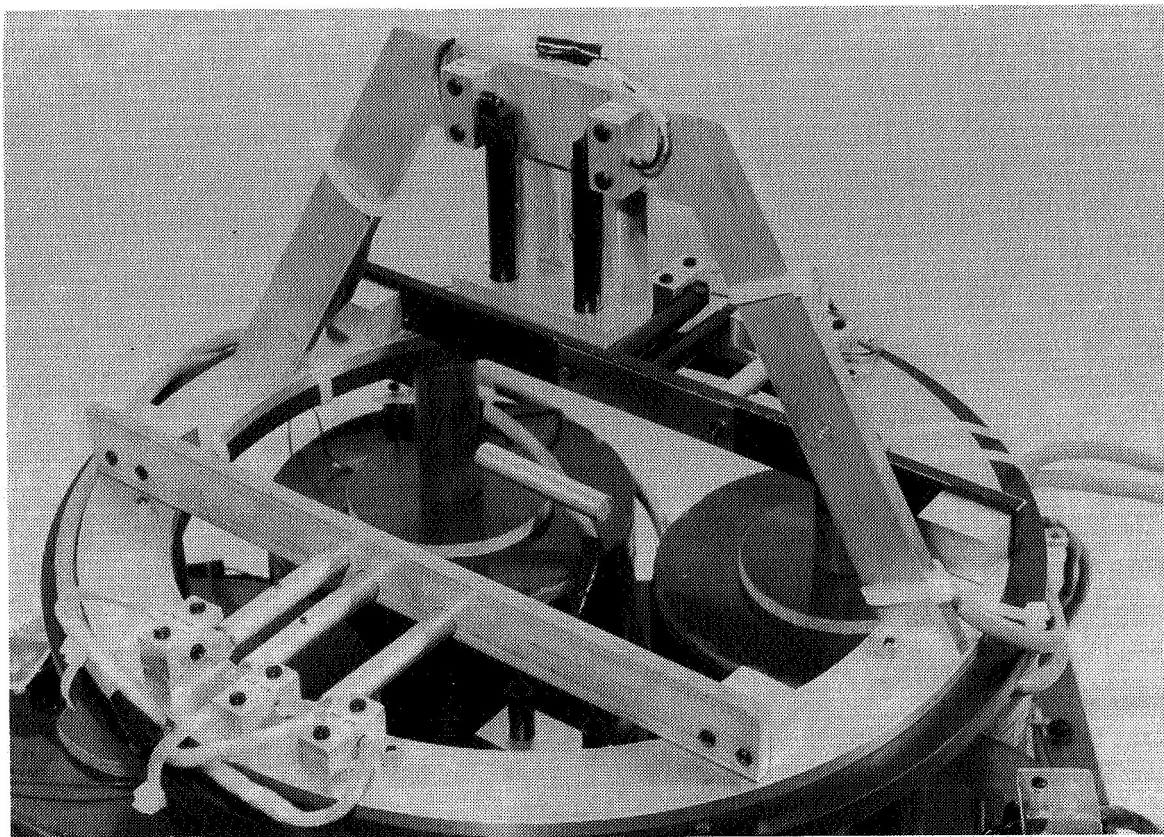


Figure 9 - LAMSTF Operating with Analog Controller

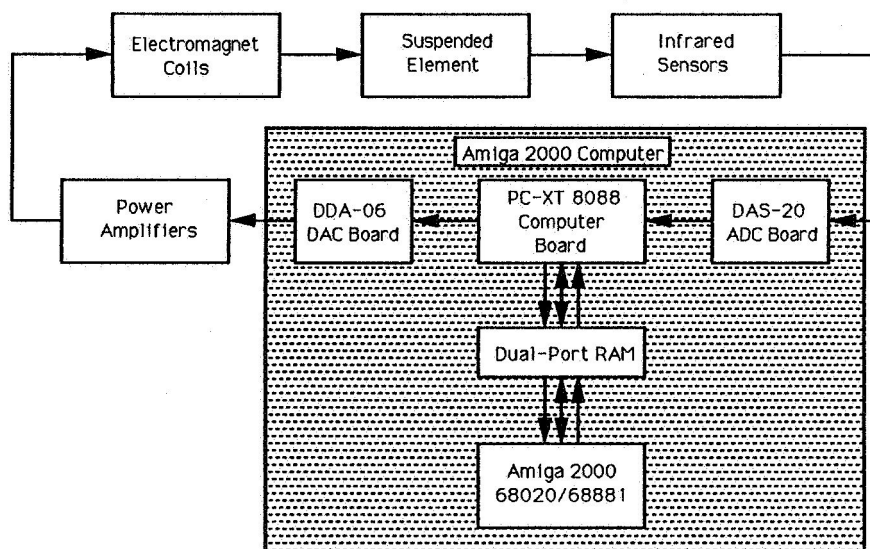


Figure 10 - Digital Controller Block Diagram